Single top quark production as a probe of anomalous $tq\gamma$ and tqZ couplings at the FCC-ee

Hamzeh Khanpour[1,2],[*] Sara Khatibi[2],[†] Morteza Khatiri Yanehsari[3],[‡] and Mojtaba Mohammadi Najafabadi[2§]

[(1)] *Department of Physics, University of Science and Technology of Mazandaran, P.O.Box 48518-78195, Behshahr, Iran*

[(2)] *School of Particles and Accelerators, Institute for Research in Fundamental Sciences (IPM), P.O.Box 19395-5531, Tehran, Iran*

[(3)] *School of Physics, Institute for Research in Fundamental Sciences (IPM), P.O.Box 19395-5531, Tehran, Iran*

(Dated: March 31, 2017)

In this paper, a detailed study to probe the top quark Flavour-Changing Neutral Currents (FCNC) $tq\gamma$ and tqZ at the future e^-e^+ collider FCC-ee in three different center-of-mass energies of 240, 350 and 500 GeV is presented. A set of useful variables are proposed and used in a multivariate technique to separate signal $e^-e^+ \to Z/\gamma \to t\bar{q}$ ($\bar{t}q$) from standard model background processes. The study includes a fast detector simulation based on the DELPHES package to consider the detector effects. The 3σ discovery regions and the upper limits on the FCNC branching ratios at 95% confidence level (CL) in terms of the integrated luminosity are presented. It is shown that with 300 fb^{-1} of integrated luminosity of data, FCC-ee would be able to exclude the effective coupling strengths above $\mathcal{O}(10^{-4} - 10^{-5})$ which is corresponding to branching fraction of $\mathcal{O}(0.01 - 0.001)\%$. We show that moving to a high-luminosity regime leads to a significant improvement on the upper bounds on the top quark FCNC couplings to a photon or a Z boson.

PACS numbers: 12.38.Bx, 12.39.-x, 14.65.Bt

[*] Hamzeh.Khanpour@mail.ipm.ir
[†] S.Khatibi@ipm.ir
[‡] Khatiri@ipm.ir
[§] Mojtaba@ipm.ir

CONTENTS

I. INTRODUCTION

The top quark with its large mass and very short life time is one of the most interesting discovered particles in the Standard Model (SM). Studying the top quark enables us to investigate the electroweak symmetry breaking mechanism (EWSB) as well as searching for extensions of the SM. In the framework of the SM, top-quark Flavour-Changing Neutral Currents (FCNC) only arise at loop level and are highly suppressed because of the GIM (Glashow-Iliopoulos-Maiani) mechanism [1]. For instance, the SM predictions for the branching fractions of FCNC processes like $t \to \gamma u(c)$ and $t \to Zu(c)$ are of the order of $10^{-16}(10^{-14})$ and $10^{-17}(10^{-14})$, respectively [2]. The ability of the present experiments is far from measuring such tiny branching ratios. On the other hand, several extensions of the SM such as Technicolor, SUSY models, Higgs doublet models predict much higher branching ratios up to $10^8 - 10^{10}$ order of magnitude larger than SM predictions [2–8]. Consequently, any observation of these rare FCNC transitions would be a clear signal of new physics beyond the SM.

So far, there are several experimental studies in searching for FCNC transitions of the top quark to a photon or a Z boson through different channels [9–24]. The most stringent observed upper

limits at 95% confidence level (CL) have been found to be [9, 11, 25]:

$$\begin{aligned}
\text{CMS}: & Br(t \to Zu) < 0.017\%\,, \\
& Br(t \to Zc) < 0.020\%\,, \\
\text{ATLAS}: & Br(t \to Zq) < 0.07\%\ \text{(observed)}\,, \\
& Br(t \to Zq) < 0.08\%\ \text{(expected)}\,, \\
\text{CMS}: & Br(t \to u\gamma) < 0.013\%\,, \\
& Br(t \to c\gamma) < 0.170\%\,. \qquad (1)
\end{aligned}$$

It is notable that even at the future upgrades of the LHC, these bounds would not be improved considerably. For example, the future upper bounds on $Br(t \to qZ)$ have been predicted to be 0.01% at 95% CL at 14 TeV center-of-mass energy with 3000 fb^{-1} of integrated luminosity of data [26, 27]. The branching fraction of $Br(t \to q\gamma)$ would be reachable down to 10^{-4} for $q = c$ and 10^{-5} for $q = u$ at the integrated luminosity of 3000 fb^{-1} at the LHC [28]. Therefore, an important task is to look at the future colliders potential to search for the anomalous FCNC couplings, in particular the e^-e^+ colliders such as International Linear Collider (ILC) [29–36], Compact Linear Collider (CLIC) [37–40], Circular Electron-Positron Collider (CEPC) [41, 42] and the high-luminosity high-precision Future Circular Collider (FCC-ee) [43–52].

In Refs. [53, 54], an analysis has been performed to probe the sensitivity of a future e^-e^+ collider to top quark FCNC to the photon and a Z boson in the $e^-e^+ \to Z/\gamma \to t\overline{q}$ ($\overline{t}q$) channel. This analysis has been done at the center-of-mass energies of 500 GeV and 800 GeV with the integrated luminosity of up to 1 ab^{-1} without including the effects of parton showering, hadronization, and decay of unstable particles. However, the analysis considers cases with and without the beam polarization to estimate the sensitivity to $tq\gamma$ and tqZ FCNC couplings.

The future large scale circular electron-positron collider (FCC-ee) would be one of the high-precision and high-luminosity machines which will be able to perform precise measurements on the Higgs boson, top-quark, Z and W bosons [43, 55]. Due to the expected large amount of data and large production rates, FCC-ee can provide an excellent opportunity for precise studies, in particular in the top quark sector. FCC-ee is designed to be working at the center-of-mass energy up to the $t\bar{t}$ threshold mass, i.e. $\sqrt{s} = 350$ GeV which is upgradeable to 500 GeV. The goal is to reach to a luminosity of $L = 1.3 \times 10^{34}$ cm^{-2}s^{-1} [43, 55].

In this paper, our aim is to study the anomalous FCNC of $tq\gamma$ and tqZ via single top quark production in the FCC-ee at three different center-of-mass energies of 240 GeV, 350 GeV and 500

GeV. The final state consists of a top quark in association with a light-quark. We consider the leptonic decay of the W boson in top quark decay, ($t \to Wb \to \ell\nu_\ell b$, where $\ell = e, \mu$). In the analysis, we perform parton shower, hadronization and decays of unstable particles as well as the detector effects. We present the 3σ discovery ranges and upper limits on the branching ratios at 95% C.L in terms of the integrated luminosity. Finally, the results are compared with the present and future results from the LHC experiments.

The paper is organized as follows. In Section II, we present the theoretical framework which describes the top quark FCNC couplings to a photon and a Z boson. The Monte Carlo event generation, detector simulation and signal separation from backgrounds are described in Section III. In Section IV, the results of the sensitivity estimation are presented. Finally, Section V concludes the paper.

II. THEORETICAL FORMALISM

The anomalous FCNC couplings of a top quark with a photon and a Z boson can be written in a model independent way using an effective Lagrangian approach. The lowest order terms describing $tq\gamma$ and tqZ couplings have the following form [21, 54, 56–58]:

$$\begin{aligned}\mathcal{L}_{\text{eff}} = \sum_{q=u,c} \Bigg[& e\lambda_{tq}\bar{t}(\lambda^v - \lambda^a\gamma^5)\frac{i\sigma_{\mu\nu}q^\nu}{m_t}qA^\mu \\ & + \frac{g_W}{2c_W}\kappa_{tq}\bar{t}(\kappa^v - \kappa^a\gamma^5)\frac{i\sigma_{\mu\nu}q^\nu}{m_t}q\ Z^\mu \\ & + \frac{g_W}{2c_W}X_{tq}\ \bar{t}\gamma_\mu(x^L P_L + x^R P_R)q\ Z^\mu \Bigg] + \text{h.c.}\,,\end{aligned} \tag{2}$$

where λ_{tq}, κ_{tq} and X_{tq} are dimensionless real parameters that denote the strength of the anomalous FCNC couplings. In the above effective Lagrangian, the chirality parameters are normalized to $|\lambda^a|^2 + |\lambda^v|^2 = |x^L|^2 + |x^R|^2 = |\kappa^v|^2 + |\kappa^a|^2 = 1$ and $P_{L,R}$ are the left- and right-handed projection operators, $P_{L,R} = \frac{1}{2}(1 \mp \gamma^5)$. The anomalous FCNC interactions $tq\gamma$ and tqZ lead to production of a top quark in association with a light quark in electron-positron collisions. The Feynman diagram for this process is shown in Figure 1 including the subsequent leptonic decay of the W boson in the top quark decay. In Table I, the cross sections of $e^- + e^+ \to t\bar{u} + t\bar{c} + \bar{t}u + \bar{t}c$ including the branching ratio of the top quark decays into a W boson and a b-quark, and W boson decays into a charged lepton (muon and electron) and a neutrino are presented. The cross sections are shown at three different center-of-mass energies of 240, 350 and 500 GeV. It should be pointed out that the cross sections due to photon and Z boson exchange are different and depends on the type of FCNC

coupling. The contribution of photon and Z boson exchange with the $\sigma^{\mu\nu}$ coupling increases with the energy of the center-of-mass. This is because of the presence of an additional momentum factor q^{ν} in the effective Lagrangian.

According to the three independent terms of the Lagrangian, there are three separate ways to produce single top quark plus a light quark. In this analysis, all three terms of the Lagrangian are investigated independently with the following sets of the chirality parameters: $\lambda^v = 1, \lambda^a = 0$ for $tq\gamma$, for vector like coupling of tqZ: $x^L = x^R$ while for tensor FCNC coupling of tqZ: $\kappa^v = 1, \kappa^a = 0$. In case of observing an excess indicating FCNC signal, the angular distribution of the outgoing particles can be used to determine the chirality of the FCNC couplings. In Figure 2, the distributions of the cosine of the angle between the outgoing charged lepton with respect to the $z-$axis (beam axis) are depicted for the $tq\gamma$ signal scenario with three independent types of couplings: $(\lambda^v = 1, \lambda^a = 0)$, $(\lambda^v = 1, \lambda^a = 1)$ and $(\lambda^v = 1, \lambda^a = -1)$ at $\sqrt{s} = 240$ GeV. As it can be seen, for the type of coupling with no γ^5 the angular distribution is quite flat while for the type of coupling with projection operator $1 \pm \gamma^5$, the distribution has a behavior like a parabola with opposite shapes depending on the sign of γ^5.

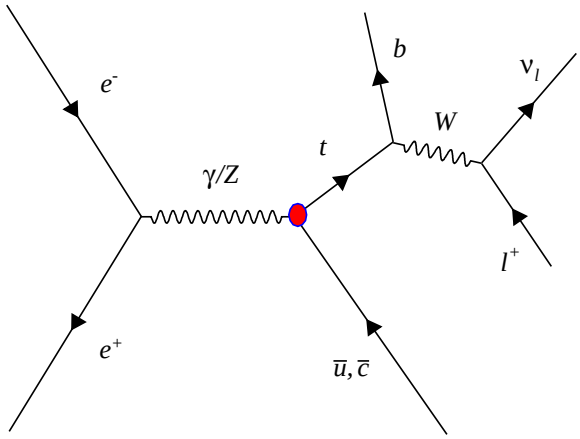

Figure 1: The Feynman diagram for production of a top in association with a light quark due to the anomalous couplings $tq\gamma$ and tqZ in electron-positron collisions.

III. ANALYSIS STRATEGY

As we have mentioned before, this study is dedicated to probe the $tq\gamma$ and tqZ FCNC couplings via single top quark production at FCC-ee. The results will be presented at different center-of-mass energies of the colliding electron-positron. In this section, the details of the event generation and

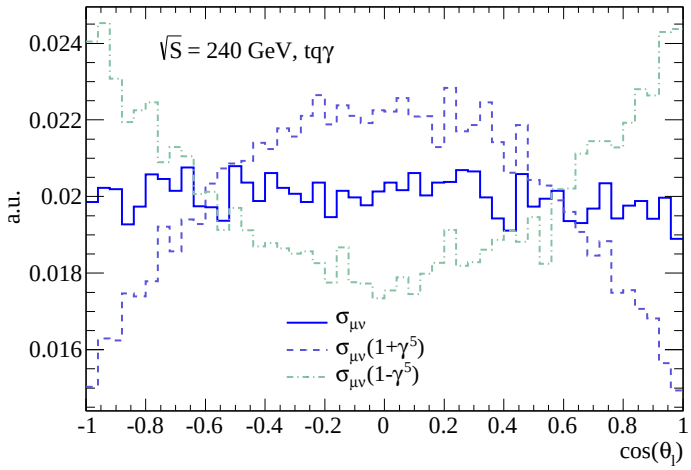

Figure 2: The distribution of the cosine of the angle between the outgoing charged lepton with the $z-$axis for $tq\gamma$ with different chirality assumptions at the center-of-mass energy of 240 GeV.

$\sqrt{s}$	240 GeV	350 GeV	500 GeV
FCNC coupling	σ(fb)	σ(fb)	σ(fb)
$tq\gamma$	$2154(\lambda_{tq})^2$	$3832(\lambda_{tq})^2$	$4302(\lambda_{tq})^2$
tqZ $(\sigma_{\mu\nu})$	$1434(\kappa_{tq})^2$	$2160(\kappa_{tq})^2$	$2282(\kappa_{tq})^2$
tqZ (γ_{μ})	$916(X_{tq})^2$	$786(X_{tq})^2$	$464(X_{tq})^2$

Table I: Cross-sections (in fb) of $\sigma(e^- + e^+ \to t\bar{u} + t\bar{c} + \bar{t}u + \bar{t}c) \times Br(t \to Wb \to l\nu b)$ with $\ell = e, \mu$ for three signal scenarios, $tq\gamma$, tqZ (vector-tensor) before applying any cut.

Monte Carlo simulation for signal and backgrounds, event selection, and multivariate analysis to separate signal process from SM background processes will be presented.

A. Event generation and simulation

The signal process is defined as $e^-e^+ \to Z/\gamma \to t\bar{q}$ $(\bar{t}q)$, where q is an up or a charm quark. The top quark decays through SM, $t \to W^+b \to \ell^+\nu_\ell b$ and $\bar{t} \to W^-\bar{b} \to \ell^-\overline{\nu}_\ell\bar{b}$. Therefore, the final state consists of a charged lepton, missing energy, a b-jet and a light jet.

In order to simulate and generate the signal events, the effective Lagrangian describing the FCNC couplings is implemented with the FeynRules package [59–63], then the model has been imported to a UFO module [64] and inserted in MadGraph 5 package [65, 66].

Based on the expected signature of the signal process, the main background contribution is

originating from $W^{\pm}jj$ production when the W boson decays leptonically, i.e. $e^+e^- \to W^{\pm}jj \to \ell^+\nu_\ell jj(\ell^-\overline{\nu}_\ell jj)$. Other backgrounds to the signal include the $t\bar{t}$ events in semi-leptonic channel and $Z\ell^{\pm}\ell^{\pm}$ (with hadronic decay of the Z boson). All of these backgrounds are generated at leading order with MadGraph 5. The cross sections of the background processes at the center-of-mass energies of $\sqrt{s} = 240$, 350 and 500 GeV are presented in the first row of Tables II, III, IV.

We employ Pythia 8.1 package [67–70] for parton showering, hadronization and decay of unstable particles. To reconstruct jets the FastJet package [71–73] with an anti-k_t algorithm [74, 75] with a cone size of 0.5 is used. Then the delphes 3 package [76, 77] is employed to model the detector performance. We present the results with 70% for the efficiency of b-tagging, a mistagging rate of 10% for charm-quark jets and 1% for other light-flavor jets. It will be shown that the b-tagging requirement plays an important role to reject the background contributions, in particular, $W^{\pm}jj$ and $Z\ell^{\pm}\ell^{\pm}$.

The jet energies are smeared in delphes similar to an ILD-like detector [31, 78, 79]

$$\frac{\Delta E_j}{E_j} = \frac{30\%}{\sqrt{E_j\ (\text{GeV})}}\,, \tag{3}$$

The detector performance modeling of leptons (electrons and muons) is taken similar to a CMS-like detector which has been described in Ref. [80].

Events are preselected by requiring only one charged lepton (electron or muon) with $p_T^{\ell} \geq 10$ GeV and $|\eta^{\ell}| < 2.5$. No specific requirement is applied as for trigger condition however the presence of an energetic charged lepton is assumed to be enough. We require to have at least two jets in each event with $p_T^{jet} \geq 10$ GeV and $|\eta^{jet}| < 2.5$, from which one is required to be originating from the hadronization of a b-quark. The events are rejected in which the charged leptons are not isolated. In this analysis, the events with at least one b-tagged jet are kept and the total number of jets is required to be greater than two. These requirements with the preliminary requirement of the presence of only one isolated charged lepton in the final state help suppress the contribution of background events from the top quark pair production. Among the non-b-tagged jets, the one with highest transverse momentum is chosen to be originating from the light quark in the final state. The four-momentum of the neutrino is determined without any ambiguity from the missing momentum of the event. The missing momentum is required be greater than 10 GeV. To reconstruct the signal topology, first the W boson momentum is reconstructed from the momenta of the charged lepton and the neutrino as $p_W = p_l + p_\nu$. The top quark four-momentum is obtained by combining the reconstructed W boson with the b-tagged jet. The mass distribution of the reconstructed top quark is illustrated in Figure 3 for $tq\gamma$ signal and for background processes $W^{\pm}jj$, $t\bar{t}$ and $Z\ell^{\pm}\ell^{\pm}$.

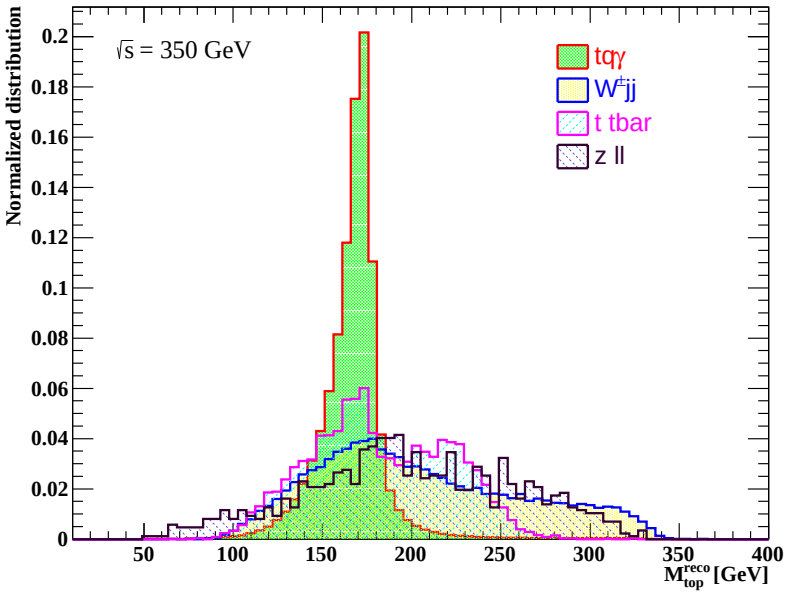

Figure 3: The normalized reconstructed top quark mass distributions for signal ($tq\gamma$) and the corresponding $W^{\pm}jj$, $t\bar{t}$ and $Z\ell^{\pm}\ell^{\pm}$ SM background processes at $\sqrt{s} = 350$ GeV. The signal has been shown with $\lambda_{tq} = 0.1$.

The distribution is at the center-of-mass energy of 350 GeV. As expected the reconstructed top quark mass distribution for signal has a peak around the top quark mass while the background processes have an almost flat distribution with no sharp peak. The top quark pair background process also has an almost sharp peak on the top quark mass due to the fact that the charged lepton, neutrino, and b-jet are coming from one of the top quarks. The $W^{\pm}jj$ background has a broad invariant mass distribution because the b-jet candidate is not originating from the decay of a top quark.

B. Separation of signal from background

In order to reduce the SM background processes which have different topologies from the signal events, a multivariate technique [81–85] is used. After the preselection cuts described in the previous section which consists of the detector acceptance cuts, and including the effects of b-tagging and mistagging, around 40–45% of the signal events and 1–4% of background events are survived. The cross sections of signal in all scenarios and the corresponding SM backgrounds at three center-of-mass energies after the preselection cuts are presented in Table II, III and IV for $\sqrt{s} = 240$, 350

and 500 GeV, respectively.

$\sqrt{s} = 240GeV$	Signal			Background	
Cuts	$tq\gamma$	tqZ $(\sigma_{\mu\nu})$	tqZ (γ_μ)	$W^\pm jj$	$Z\ell^\pm\ell^\pm$
Cross-sections (in fb)	$2154.0(\lambda_{tq})^2$	$1434.0(\kappa_{tq})^2$	$916.0(X_{tq})^2$	4881.2	3588.4
$1\ell + \lvert\eta^\ell\rvert < 2.5 + P_T^\ell > 10 + \lvert\vec{p}_{\rm miss}\rvert > 10$	$1679.8(\lambda_{tq})^2$	$1117.8(\kappa_{tq})^2$	$715.6(X_{tq})^2$	3886.3	100.1
$\geq 2jets + \lvert\eta^{jets}\rvert < 2.5 + P_T^{jets} > 10$	$1393.3(\lambda_{tq})^2$	$927.3(\kappa_{tq})^2$	$590.9(X_{tq})^2$	3459.1	59.7
$n_{b-jet} \geq 1$	$900.5(\lambda_{tq})^2$	$598.7(\kappa_{tq})^2$	$381.8(X_{tq})^2$	185.3	15.3

Table II: Cross-sections (in fb) for the three signal scenarios, $tq\gamma$, tqZ (vector and tensor) and the corresponding $W^\pm jj$ and $Z\ell^\pm\ell^\pm$ SM backgrounds passing sequential cuts at $\sqrt{s} = 240$ GeV.

$\sqrt{s} = 350GeV$	Signal			Background		
Cuts	$tq\gamma$	tqZ $(\sigma_{\mu\nu})$	tqZ (γ_μ)	$W^\pm jj$	$t\bar{t}$	$Z\ell^\pm\ell^\pm$
Cross-sections (in fb)	$3832.0(\lambda_{tq})^2$	$2160.0(\kappa_{tq})^2$	$786.0(X_{tq})^2$	3221.1	62.53	4085.0
$1\ell + \lvert\eta^\ell\rvert < 2.5 + P_T^\ell > 10 + \lvert\vec{p}_{\rm miss}\rvert > 10$	$2984.2(\lambda_{tq})^2$	$1680.2(\kappa_{tq})^2$	$614.6(X_{tq})^2$	2447.6	40.5	129.5
$\geq 2jets + \lvert\eta^{jets}\rvert < 2.5 + P_T^{jets} > 10$	$2499.1(\lambda_{tq})^2$	$1405.6(\kappa_{tq})^2$	$507.9(X_{tq})^2$	2175.5	0.65	77.7
$n_{b-jet} \geq 1$	$1614.1(\lambda_{tq})^2$	$909.0(\kappa_{tq})^2$	$328.4(X_{tq})^2$	112.4	0.43	20.3

Table III: Cross-sections (in fb) for three signal scenarios, $tq\gamma$, tqZ (vector and tensor) and the corresponding $W^\pm jj$, $t\bar{t}$ and $Z\ell^\pm\ell^\pm$ SM backgrounds passing sequential cuts at at $\sqrt{s} = 350$ GeV.

$\sqrt{s} = 500GeV$	Signal			Background		
Cuts	$tq\gamma$	tqZ $(\sigma_{\mu\nu})$	tqZ (γ_μ)	$W^\pm jj$	$t\bar{t}$	$Z\ell^\pm\ell^\pm$
Cross-sections (in fb)	$4302.0(\lambda_{tq})^2$	$2282.0(\kappa_{tq})^2$	$464.0(X_{tq})^2$	2048.8	148.7	4070.0
$1\ell + \lvert\eta^\ell\rvert < 2.5 + P_T^\ell > 10 + \lvert\vec{p}_{\rm miss}\rvert > 10$	$3277.3(\lambda_{tq})^2$	$1736.9(\kappa_{tq})^2$	$355.1(X_{tq})^2$	1383.7	106.9	144.7
$\geq 2jets + \lvert\eta^{jets}\rvert < 2.5 + P_T^{jets} > 10$	$2757.8(\lambda_{tq})^2$	$1460.8(\kappa_{tq})^2$	$292.0(X_{tq})^2$	1242.1	1.38	89.7
$n_{b-jet} \geq 1$	$1776.9(\lambda_{tq})^2$	$941.9(\kappa_{tq})^2$	$188.0(X_{tq})^2$	60.9	0.89	24.3

Table IV: Cross-sections (in fb) for the three signal scenarios, $tq\gamma$, tqZ (vector and tensor) and the corresponding $W^\pm jj$, $t\bar{t}$ and $Z\ell^\pm\ell^\pm$ SM backgrounds passing sequential cuts at $\sqrt{s} = 500$ GeV.

These preselection cuts are generally loose on a single variable and remove a large fraction of the background events while barely reducing also the signal events. In order to obtain a better separation of signal from background events, a multivariate technique is used. The choice of proper set of variables is important in keeping the signal events, while reducing the large fraction of SM

background events. We select those variables which have the best possible discrimination power between signal and background processes. The following variables are used in the analysis:

- $\Delta R(\ell, \mathrm{b-jet})$: the angular separation between the lepton and b-jet
- $p_T^{\mathrm{b-jet}}, \eta^{\mathrm{b-jet}}$: the transverse momentum and pseudorapidity of the b-jet
- $M_{\mathrm{top}}^{\mathrm{rec}}$: the reconstructed top quark mass
- E^{ℓ}, η^{ℓ}: the energy and pseudorapidity of the charged lepton
- P_T^{top}: the transverse momentum of reconstructed top-quark
- $E^{\mathrm{light-jet}}$: the energy of the light jet

The distributions of some of these variables are shown in Figure 4. These distributions are corresponding to the signal scenario with anomalous $tq\gamma$ coupling at the center-of-mass energy of 350 GeV. For all signal scenarios $tq\gamma$, $tqZ(\gamma^{\mu})$ and $tqZ(\sigma_{\mu\nu})$ the same variables are used as the inputs of the multivariate analyses. The analyses are performed separately at the center-of-mass energies of 240, 350 and 500 GeV. Going to higher center-of-mass energies leads to reduce the overlapping between the signal and background distributions in the MVA output.

The cross sections of the signal and the $W^{\pm}jj$, $t\bar{t}$ and $Z\ell^{\pm}\ell^{\pm}$ background processes after performing the multivariate analysis are presented in Table V. As can be seen from this table, the background rejection rate varies at different center-of-mass energies. For all signal scenarios, the background rejection rates after the multivariate analysis technique are $\sim 10^{-1}$, $\sim 10^{-2}$ and $\sim 10^{-3}$ at the center-of-mass energies of 240, 350, 500 GeV, respectively. The discriminating power of the input variables are increasing with the center-of-mass energies of the collision. Going to higher energies the overlapping between the signal and background distributions is reduced. In particular, this happens for the top mass, lepton energy and the top quark transverse momentum distributions. Larger background suppression is achieved for the tqZ signal with $\sigma_{\mu\nu}$ coupling with respect to the γ_{μ} coupling. Since the signal-to-background ratio for all signal scenarios increases with the increment of the center-of-mass energy, more sensitivity is expected at larger energies.

IV. SENSITIVITY ESTIMATION

To estimate the sensitivities, the expected 3σ significance and the upper limits on the branching ratios at 95% C.L are presented. The 3σ discovery ranges are obtained using the significance $S/\sqrt{B}$,

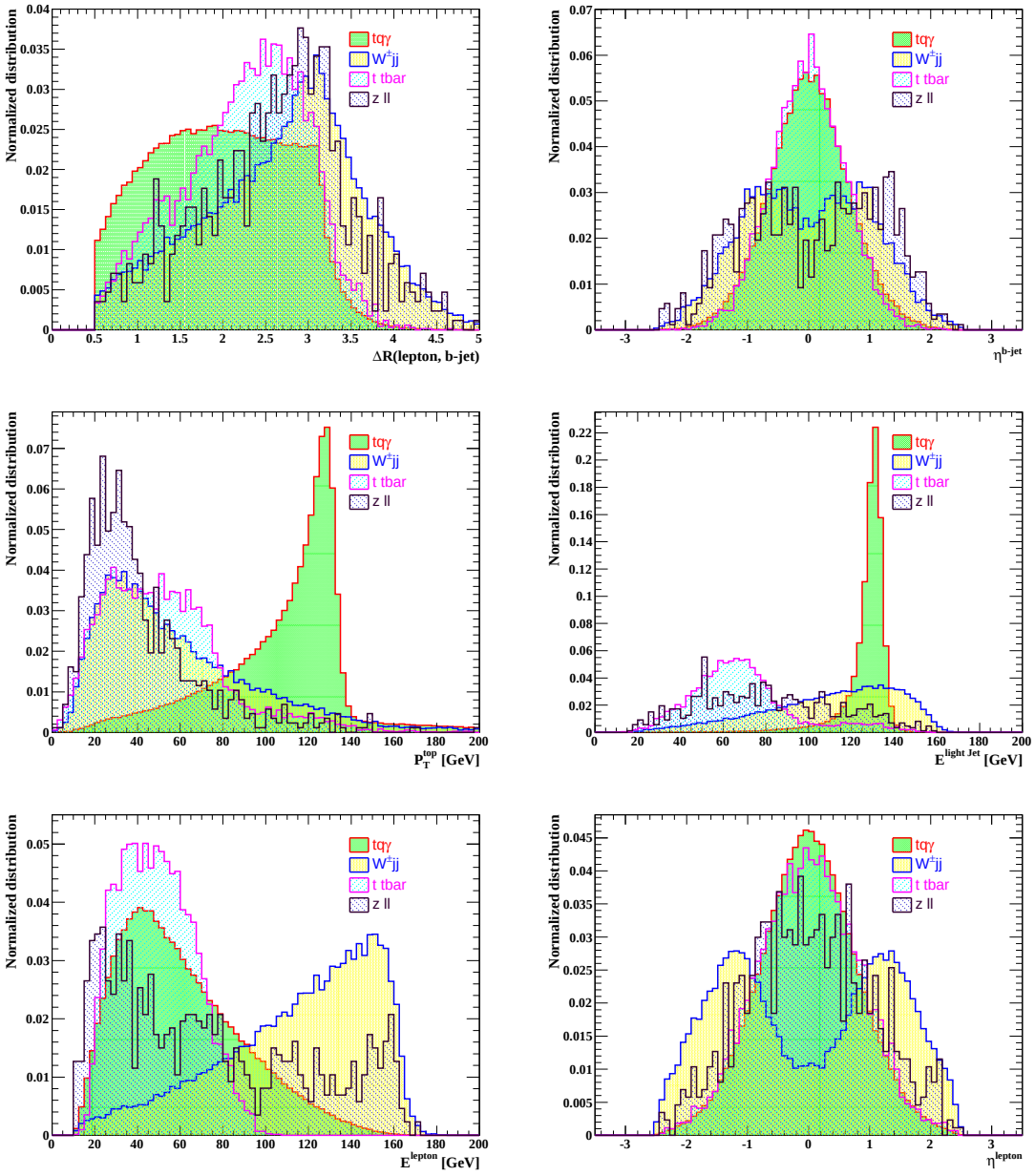

Figure 4: The normalized distributions of some of the input variables to the multivariate analysis for the the center-of-mass energy of 350 GeV.

where S and B are the number of signal and background events after all selections, respectively. Without including any systematic effects, the 3σ discovery regions of the branching ratios are presented in Table VI for three signal scenarios at three center-of-mass energies. The 3σ discovery regions in terms of the integrated luminosity are also depicted in Figure 5. We observe that at 3σ significance level branching ratios at the order of $10^{-3} - 10^{-4}$ is achievable at the center-of-mass

$\sqrt{s}$=240 GeV	Couplings	Signal	$W^{\pm}jj$ (fb)		$Z\ell^{\pm}\ell^{\pm}$ (fb)
	$tq\gamma$	$826.32(\lambda_{tq})^2$	26.59	-	5.27
TMVA	tqZ $(\sigma_{\mu\nu})$	$547.90(\kappa_{tq})^2$	25.65	-	2.15
	tqZ (γ_{μ})	$354.13(X_{tq})^2$	30.56	-	2.57
$\sqrt{s}$=350 GeV		Signal	$W^{\pm}jj$ (fb)	$t\bar{t}$ (fb)	$Z\ell^{\pm}\ell^{\pm}$ (fb)
	$tq\gamma$	$1521.31(\lambda_{tq})^2$	7.59	0.034	1.45
TMVA	tqZ $(\sigma_{\mu\nu})$	$856.72(\kappa_{tq})^2$	7.61	0.031	1.45
	tqZ (γ_{μ})	$306.48(X_{tq})^2$	8.49	0.37	1.74
$\sqrt{s}$=500 GeV		Signal	$W^{\pm}jj$ (fb)	$t\bar{t}$ (fb)	$Z\ell^{\pm}\ell^{\pm}$ (fb)
	$tq\gamma$	$1677.29(\lambda_{tq})^2$	2.11	0.11	0.64
TMVA	tqZ $(\sigma_{\mu\nu})$	$895.71(\kappa_{tq})^2$	2.43	0.14	0.64
	tqZ (γ_{μ})	$176.68(X_{tq})^2$	3.07	0.13	1.21

Table V: Cross-sections (in fb) of signal and $W^{\pm}jj$, $t\bar{t}$ and $Z\ell^{\pm}\ell^{\pm}$ background processes after performing the multivariate analysis for three signal scenarios, $tq\gamma$, tqZ (vector and tensor) at $\sqrt{s} = 240$, 350 and 500 GeV .

energy of 240 GeV while going to larger energies of 350 and 500 GeV can lead to an improvement of one order of magnitude for $tq\gamma$ and $tqZ(\sigma_{\mu\nu})$ with an integrated luminosity of 300 fb^{-1}. The FCNC transition of $t \to qZ$ with γ_{μ}-type couplings would not be measured better than 10^{-4}. According to Figure 5, going to high luminosity regime at the center-of-mass energies of 240 and 350 leads to a reach sensitivity at the order of 10^{-5}.

In order to set 95% CL upper limits on the anomalous FCNC couplings and consequently on the branching ratios, the CLs technique is used [86]. For the limits calculations the RooStats [87] package is used. The 95% C.L upper limits on the branching ratios of $t \to q\gamma$ and $t \to qZ$ at the center-of-mass energies of 240, 350 and 500 GeV are shown in Table VII based on an integrated luminosity of 300 fb^{-1}, 3 ab^{-1} and 10 ab^{-1}. As we expected, at each center-of-mass energy, the loosest limits belong to the FCNC transition of $t \to qZ$ with $\gamma_{\mu}-$type coupling (10^{-4}). We note that the larger center-of-mass energy leads to even one order of magnitude tighter bounds.

In order to investigate the sensitivity to b-tagging efficiency and miss-tagging rates, we also present the 95% C.L upper limits on the branching ratios of $t \to q\gamma$ and $t \to qZ$ for 85% of b-tagging efficiency and a 5% mistagging rates. The results correspond to the center-of-mass energy of 350 GeV for the integrated luminosity of 300 fb^{-1}. As can be seen from Table VIII, the higher b-tagging efficiency and smaller mistagging rates could improve the branching ratios by a factor

Integrated luminosity	Branching ratio	240 GeV	350 GeV	500 GeV
300 fb^{-1}	$Br(t \to q\gamma)$	6.38×10^{-4}	1.70×10^{-4}	1.13×10^{-4}
	$Br(t \to qZ)$ $(\sigma_{\mu\nu})$	7.85×10^{-4}	2.46×10^{-4}	1.86×10^{-4}
	$Br(t \to qZ)$ (γ_{μ})	1.50×10^{-3}	9.03×10^{-4}	1.23×10^{-3}
3 ab^{-1}	$Br(t \to q\gamma)$	2.01×10^{-4}	5.39×10^{-5}	3.58×10^{-5}
	$Br(t \to qZ)$ $(\sigma_{\mu\nu})$	2.48×10^{-4}	7.79×10^{-5}	5.90×10^{-5}
	$Br(t \to qZ)$ (γ_{μ})	4.73×10^{-4}	2.85×10^{-4}	3.91×10^{-4}
10 ab^{-1}	$Br(t \to q\gamma)$	2.01×10^{-5}	2.95×10^{-5}	1.96×10^{-5}
	$Br(t \to qZ)$ $(\sigma_{\mu\nu})$	2.44×10^{-5}	4.27×10^{-5}	3.23×10^{-5}
	$Br(t \to qZ)$ (γ_{μ})	2.59×10^{-4}	1.56×10^{-4}	2.14×10^{-4}

Table VI: The sensitivity for a significance level of 3σ at the center-of-mass energies of 240, 350, 500 GeV for the integrated luminosities of 300 fb^{-1}, 3 ab^{-1}, 10 ab^{-1}.

Integrated luminosity	Branching ratio	240 GeV	350 GeV	500 GeV
300 fb^{-1}	$Br(t \to q\gamma)$	1.23×10^{-4}	3.43×10^{-5}	2.45×10^{-5}
	$Br(t \to qZ)$ $(\sigma_{\mu\nu})$	1.50×10^{-4}	4.97×10^{-5}	3.94×10^{-5}
	$Br(t \to qZ)$ (γ_{μ})	3.06×10^{-4}	1.83×10^{-4}	2.67×10^{-4}
3 ab^{-1}	$Br(t \to q\gamma)$	3.70×10^{-5}	9.86×10^{-6}	6.76×10^{-6}
	$Br(t \to qZ)$ $(\sigma_{\mu\nu})$	4.50×10^{-5}	1.41×10^{-5}	1.09×10^{-5}
	$Br(t \to qZ)$ (γ_{μ})	9.25×10^{-5}	5.27×10^{-5}	7.49×10^{-4}
10 ab^{-1}	$Br(t \to q\gamma)$	2.01×10^{-5}	5.25×10^{-6}	3.59×10^{-6}
	$Br(t \to qZ)$ $(\sigma_{\mu\nu})$	2.44×10^{-5}	7.60×10^{-6}	5.85×10^{-6}
	$Br(t \to qZ)$ (γ_{μ})	5.02×10^{-5}	2.83×10^{-5}	4.00×10^{-5}

Table VII: The upper limits on the top FCNC decays at 95% C.L obtained at the center-of-mass energies of 240, 350 and 500 GeV for the integrated luminosities of 300 fb^{-1}, 3 ab^{-1}, 10 ab^{-1}.

of around 1.6. Charm-tagging algorithm could leads to distinguish between tuV and tcV FCNC interactions. It is found that a charm tagging algorithm with an efficiency of 30% provides the possibility to separate tuV and tcV and branching fractions of $t \to c\gamma$ down to 10^{-5} with an integrated luminosity of 10 ab^{-1} at the center-of-mass energy of 240 GeV is achievable.

The effect of systematic uncertainties is considered for two assumed values of overall uncertainties: 5% and 10%. The change on the branching fraction of $Br(t \to q\gamma)$, ΔBr, are 0.50×10^{-5} and

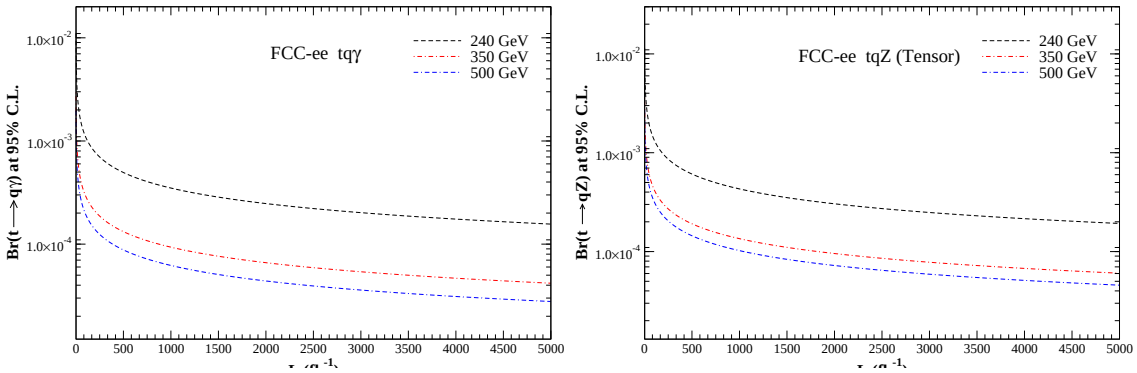

(a)

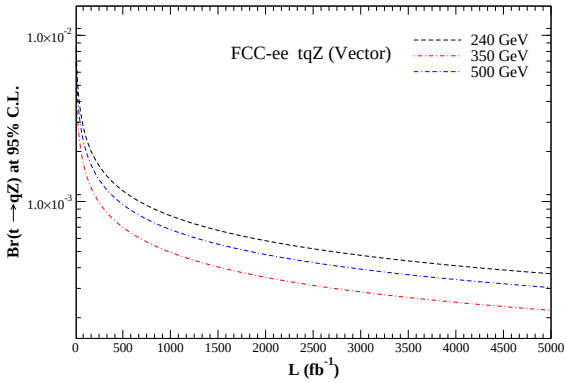

(c)

Figure 5: Branching ratios of a FCNC signal detectable at the 3σ level as a function of integrated luminosity at $\sqrt{s}$ = 240, 350 and 500 GeV of FCC-ee energies. (a) for $Br(t \to q\gamma)$, (b) for $Br(t \to qZ)$ $(\sigma_{\mu\nu})$, and (c) for $Br(t \to qZ)$ (γ_μ).

5.47×10^{-5} for the uncertainties of 5% and 10%, respectively.

$\sqrt{s}$	$Br(t \to q\gamma)$	$Br(t \to qZ)$ $(\sigma_{\mu\nu})$	$Br(t \to qZ)$ (γ_μ)
350 GeV	2.19×10^{-5}	3.12×10^{-5}	1.22×10^{-4}

Table VIII: The upper limits on the top FCNC decays at 95% C.L obtained using the CLs method at the $\sqrt{s}$ = 350 GeV for 85% of b-tagging efficiency and a 5% mistagging rates based on an integrated luminosity of 300 fb^{-1}.

In Figure 6, we present the current observed upper limits on the $Br(t \to qZ)$ versus $Br(t \to q\gamma)$ at 95% CL from CMS experiments [11, 25]. The expected sensitivity from the CMS experiment with 3000 fb^{-1} in proton-proton collisions at the center-of-mass energy of 14 TeV is also shown [28]. The sensitivity of the FCC-ee with 3 ab^{-1} at the center-of-mass energy of 350 GeV, and with 10

ab^{-1} at the center-of-mass energy of 240 GeV are compared with the CMS experiment results. With an integrated luminosity of 3000 fb^{-1}, CMS is expected to reach to an upper limit of 2.7×10^{-5} on the branching ratio of $t \to u\gamma$, 2.0×10^{-4} on the branching ratio of $t \to c\gamma$, and 1.0×10^{-4} on the branching ratio of $t \to qZ$ ($\sigma_{\mu\nu}-$type coupling). The FCC-ee potential upper limits are expected to be significantly smaller than the expected limits by the future LHC program.

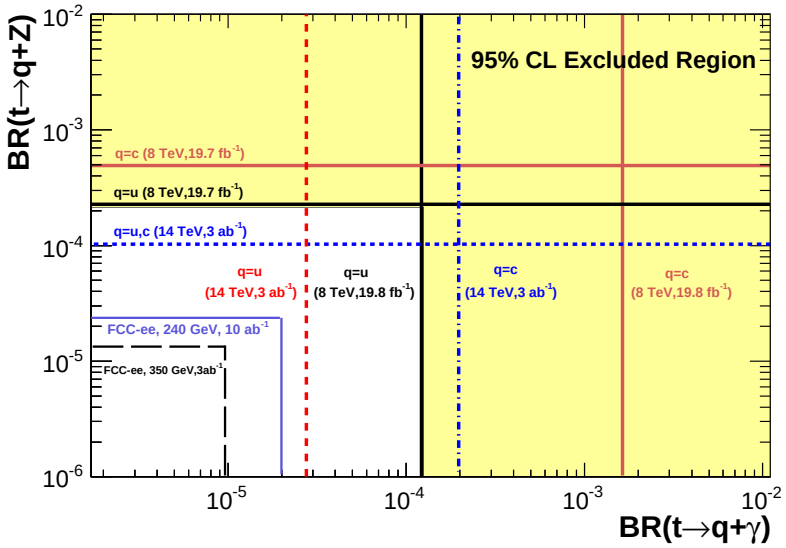

Figure 6: The current observed upper limits on the $Br(t \to qZ)$ versus $Br(t \to q\gamma)$ at 95% C.L from the recent analyses of the CMS experiment [11, 25]. The expected sensitivity from the CMS experiment with 3000 fb^{-1} is also shown [28]. The sensitivity of the FCC-ee with 3 ab^{-1} at the center-of-mass energy of 350 GeV, and with 10 ab^{-1} at the center-of-mass energy of 240 GeV are presented as well.

It is worth mentioning that the FCNC transitions can also be probed in $t\bar{t}$ production when a top quark decays anomalously into $q+\gamma$ or $q+Z$. However, it has been found that the limits would be looser than the ones obtained in single top productions [53]. In case of signal observation, LHC would also be able to discriminate between anomalous tuV and tcV ($V = \gamma, Z$) using the charge ratio technique [88]. As we already discussed, this would be possible at the FCC-ee by having an efficient of charm tagging technique.

V. SUMMARY AND CONCLUSIONS

Top quark flavor-changing neutral current interactions are extremely forbidden in the SM framework because of the GIM mechanism. The SM predictions for branching ratios of the top quark decay into a photon or a Z boson and an up-type quark are at the order of 10^{-14}. However, sev-

eral extensions of the SM can enhance the branching ratios by a factor of 10^{8-9} depending on the model. Therefore, precise measurement of these branching ratios provide an excellent possibility to probe new physics beyond the SM in the top quark sector. While it is impossible to measure the branching ratios with the precisions of order of 10^{-14} to test the SM, observation of sizable branching ratios would indicate new physics beyond the SM. FCC-ee with a clean environment and high luminosity would provide a unique opportunity to measure the properties of top quark and its interactions. In this work, we have investigated the sensitivity and discovery prospects of FCC-ee to the top quark FCNC transitions. We have looked for the FCNC $tq\gamma$ and tqZ couplings in single top-quark production in the process of $e^- + e^+ \to t\bar{q} + \bar{t}q$. We perform the analysis in a model independent way using the effective Lagrangian approach at the center-of-mass energies of $\sqrt{s} =$ 240, 350 and 500 GeV. In the analysis, we only consider the leptonic (electron and muon) decay of the W boson in the top quark decay. The DELPHES package has been employed to account for the detector modeling. The main background contribution is coming from $W^{\pm}jj$ production when the W boson decays leptonically, i.e. $e^+e^- \to W^{\pm}jj \to \ell^+\nu_\ell jj(\ell^-\overline{\nu}_\ell jj)$. Other considered backgrounds in this analysis include the top quark pair events in semileptonic decay mode and $Z\ell^{\pm}\ell^{\pm}$ (with hadronic decay of Z). A set of kinematic variables has been proposed as the input variables to a multivariate analysis for discrimination of signal from background processes. We find the 3σ discovery ranges and the upper limits at 95% CL for three signal scenarios versus the integrated luminosity at the center-of-mass energies of 240, 350 and 500 GeV. We find that with increasing the center-of-mass energy stronger bounds would be reachable. With an integrated luminosity of 300 fb^{-1} at the center-of-mass energy of 350 GeV, upper limits of 3.43×10^{-5}, 4.97×10^{-5} would be obtained on $Br(t \to q\gamma)$ and $Br(t \to qZ)$ ($\sigma_{\mu\nu}-$type), respectively. A looser upper limit of 1.83×10^{-4} on $Br(t \to qZ)$ with $\gamma_\mu-$type interaction is obtained. It is found that a sensitivity of the order of 10^{-6} at high integrated luminosities would be achievable. The results of this study has been presented in the FCC-ee (TLEP) Physics Workshop (TLEP9) [89], FCC Week 2015 [90] and FCC-ee (TLEP) Physics meetings [91, 92]. We found that FCC-ee would be able to provide us stringent upper limits on the FCNC anomalous couplings and this work could serve as a base for more detailed studies in future in the FCC-ee project.

ACKNOWLEDGMENTS

The authors are grateful to Patrizia Azzi and Freya Blekman and other FCC-ee colleagues for many useful discussions and comments. Authors are thankful School of Particles and Accelera-

tors, Institute for Research in Fundamental Sciences (IPM) for financially support of this project. Hamzeh Khanpour also thanks the University of Science and Technology of Mazandaran for financial support provided for this research.

---

[1] S. L. Glashow, J. Iliopoulos and L. Maiani, Phys. Rev. D **2**, 1285 (1970). doi:10.1103/PhysRevD.2.1285

[2] K. Agashe *et al.* [Top Quark Working Group Collaboration], arXiv:1311.2028 [hep-ph].

[3] S. Bejar, J. Guasch, D. Lopez-Val and J. Sola, Phys. Lett. B **668**, 364 (2008) doi:10.1016/j.physletb.2008.09.002 [arXiv:0805.0973 [hep-ph]].

[4] J. Cao, Z. Heng, L. Wu and J. M. Yang, Phys. Rev. D **79**, 054003 (2009) doi:10.1103/PhysRevD.79.054003 [arXiv:0812.1698 [hep-ph]].
R. Guedes, R. Santos and M. Won, Phys. Rev. D **88**, no. 11, 114011 (2013) doi:10.1103/PhysRevD.88.114011 [arXiv:1308.4723 [hep-ph]].

[5] G. A. Gonzalez-Sprinberg and R. Martinez, hep-ph/0605335.
R. Coimbra, A. Onofre, R. Santos and M. Won, Eur. Phys. J. C **72**, 2222 (2012) doi:10.1140/epjc/s10052-012-2222-8 [arXiv:1207.7026 [hep-ph]].

[6] R. A. Diaz, R. Martinez and J. Alexis Rodriguez, hep-ph/0103307.

[7] G. r. Lu, F. r. Yin, X. l. Wang and L. d. Wan, Phys. Rev. D **68**, 015002 (2003) doi:10.1103/PhysRevD.68.015002 [hep-ph/0303122].

[8] G. Couture, M. Frank and H. Konig, Phys. Rev. D **56**, 4213 (1997) doi:10.1103/PhysRevD.56.4213 [hep-ph/9704305].

[9] G. Aad *et al.* [ATLAS Collaboration], Eur. Phys. J. C **76**, no. 1, 12 (2016) doi:10.1140/epjc/s10052-015-3851-5 [arXiv:1508.05796 [hep-ex]].

[10] G. Aad *et al.* [ATLAS Collaboration], Eur. Phys. J. C **76**, no. 2, 55 (2016) doi:10.1140/epjc/s10052-016-3876-4 [arXiv:1509.00294 [hep-ex]].

[11] V. Khachatryan *et al.* [CMS Collaboration], JHEP **1604**, 035 (2016) doi:10.1007/JHEP04(2016)035 [arXiv:1511.03951 [hep-ex]].

[12] Y. C. Guo, C. X. Yue and S. Yang, Eur. Phys. J. C **76**, no. 11, 596 (2016) doi:10.1140/epjc/s10052-016-4452-7 [arXiv:1603.00604 [hep-ph]].

[13] The ATLAS collaboration [ATLAS Collaboration], ATLAS-CONF-2013-063.

[14] G. Aad *et al.* [ATLAS Collaboration], JHEP **1406**, 008 (2014) doi:10.1007/JHEP06(2014)008 [arXiv:1403.6293 [hep-ex]].

[15] S. Chatrchyan *et al.* [CMS Collaboration], Phys. Lett. B **718**, 1252 (2013) doi:10.1016/j.physletb.2012.12.045 [arXiv:1208.0957 [hep-ex]].

[16] G. Aad *et al.* [ATLAS Collaboration], JHEP **1209**, 139 (2012) doi:10.1007/JHEP09(2012)139 [arXiv:1206.0257 [hep-ex]].

[17] S. Chatrchyan *et al.* [CMS Collaboration], Phys. Rev. Lett. **112**, no. 17, 171802 (2014) doi:10.1103/PhysRevLett.112.171802 [arXiv:1312.4194 [hep-ex]].

[18] Y. Chao [CMS Collaboration], PoS EPS **-HEP2013**, 069 (2013).

[19] V. M. Abazov *et al.* [D0 Collaboration], Phys. Lett. B **701**, 313 (2011) doi:10.1016/j.physletb.2011.06.014 [arXiv:1103.4574 [hep-ex]].

[20] H. Abramowicz *et al.* [ZEUS Collaboration], Phys. Lett. B **708**, 27 (2012) doi:10.1016/j.physletb.2012.01.025 [arXiv:1111.3901 [hep-ex]].

[21] V. F. Obraztsov, S. R. Slabospitsky and O. P. Yushchenko, Phys. Lett. B **426**, 393 (1998) doi:10.1016/S0370-2693(98)00260-3 [hep-ph/9712394].

[22] P. Achard *et al.* [L3 Collaboration], Phys. Lett. B **549**, 290 (2002) doi:10.1016/S0370-2693(02)02933-7 [hep-ex/0210041].

[23] J. Abdallah *et al.* [DELPHI Collaboration], Phys. Lett. B **590**, 21 (2004) doi:10.1016/j.physletb.2004.03.051 [hep-ex/0404014].

[24] CMS Collaboration [CMS Collaboration], association with a photon," CMS-PAS-TOP-14-003.

[25] CMS Collaboration [CMS Collaboration], CMS-PAS-TOP-12-039.

[26] CMS Collaboration [CMS Collaboration], CMS-PAS-FTR-13-016.

[27] [ATLAS Collaboration], ATL-PHYS-PUB-2012-001, ATL-COM-PHYS-2012-1118.

[28] CMS Collaboration [CMS Collaboration], CMS-DP-2016-064

[29] K. Fujii *et al.*, arXiv:1506.05992 [hep-ex].

[30] T. Behnke *et al.*, arXiv:1306.6329 [physics.ins-det].

[31] T. Barklow, J. Brau, K. Fujii, J. Gao, J. List, N. Walker and K. Yokoya, arXiv:1506.07830 [hep-ex].

[32] D. M. Asner *et al.*, arXiv:1310.0763 [hep-ph].

[33] G. Moortgat-Pick *et al.*, Eur. Phys. J. C **75**, no. 8, 371 (2015) doi:10.1140/epjc/s10052-015-3511-9 [arXiv:1504.01726 [hep-ph]].

[34] D. Asner, A. Hoang, Y. Kiyo, R. Pöschl, Y. Sumino and M. Vos, arXiv:1307.8265 [hep-ex].

[35] J. E. Brau, R. M. Godbole, F. R. L. Diberder, M. A. Thomson, H. Weerts, G. Weiglein, J. D. Wells and H. Yamamoto, arXiv:1210.0202 [hep-ex].

[36] M. Martinez and R. Miquel, Eur. Phys. J. C **27**, 49 (2003) doi:10.1140/epjc/s2002-01094-1 [hep-ph/0207315].

[37] L. Linssen, A. Miyamoto, M. Stanitzki and H. Weerts, doi:10.5170/CERN-2012-003 arXiv:1202.5940 [physics.ins-det].

[38] M. Aicheler *et al.*, doi:10.5170/CERN-2012-007

[39] H. Abramowicz *et al.* [CLIC Detector and Physics Study Collaboration], arXiv:1307.5288 [hep-ex].

[40] P. Lebrun *et al.*, doi:10.5170/CERN-2012-005 arXiv:1209.2543 [physics.ins-det].

[41] CEPC-SPPC Study Group, IHEP-CEPC-DR-2015-01, IHEP-TH-2015-01, IHEP-EP-2015-01.

[42] CEPC-SPPC Study Group, IHEP-CEPC-DR-2015-01, IHEP-AC-2015-01.

[43] M. Bicer *et al.* [TLEP Design Study Working Group Collaboration], JHEP **1401**, 164 (2014) doi:10.1007/JHEP01(2014)164 [arXiv:1308.6176 [hep-ex]].

[44] M. Koratzinos, PoS EPS **-HEP2015**, 518 (2015) [arXiv:1511.01021 [physics.acc-ph]].

[45] D. d'Enterria, arXiv:1602.05043 [hep-ex].

[46] J. Ellis and T. You, JHEP **1603**, 089 (2016) doi:10.1007/JHEP03(2016)089 [arXiv:1510.04561 [hep-ph]].

[47] P. Janot, JHEP **1504**, 182 (2015) doi:10.1007/JHEP04(2015)182 [arXiv:1503.01325 [hep-ph]].

[48] D. d'Enterria and P. Z. Skands, arXiv:1512.05194 [hep-ph].

[49] M. Benedikt, K. Oide, F. Zimmermann, A. Bogomyagkov, E. Levichev, M. Migliorati and U. Wienands, arXiv:1508.03363 [physics.acc-ph].

[50] M. Koratzinos *et al.*, arXiv:1506.00918 [physics.acc-ph].

[51] F. Zimmermann *et al.*, CERN-ACC-2014-0262.

[52] D. d'Enterria, Frascati Phys. Ser. **61**, 17 (2016) [arXiv:1601.06640 [hep-ex]].

[53] J. A. Aguilar-Saavedra and T. Riemann, hep-ph/0102197.

[54] J. A. Aguilar-Saavedra, Phys. Lett. B **502**, 115 (2001) doi:10.1016/S0370-2693(01)00162-9 [hep-ph/0012305].

[55] M. Koratzinos *et al.*, arXiv:1305.6498 [physics.acc-ph].

[56] E. Malkawi and T. M. P. Tait, Phys. Rev. D **54**, 5758 (1996) doi:10.1103/PhysRevD.54.5758 [hep-ph/9511337].

Y. P. Gouz and S. R. Slabospitsky, Phys. Lett. B **457**, 177 (1999) doi:10.1016/S0370-2693(99)00516-X [hep-ph/9811330].

[57] M. Hosch, K. Whisnant and B. L. Young, Phys. Rev. D **56**, 5725 (1997) doi:10.1103/PhysRevD.56.5725 [hep-ph/9703450].

J. A. Aguilar-Saavedra, Nucl. Phys. B **812**, 181 (2009) doi:10.1016/j.nuclphysb.2008.12.012 [arXiv:0811.3842 [hep-ph]].

[58] J. A. Aguilar-Saavedra, Acta Phys. Polon. B **35**, 2695 (2004) [hep-ph/0409342].

[59] A. Alloul, N. D. Christensen, C. Degrande, C. Duhr and B. Fuks, Comput. Phys. Commun. **185**, 2250 (2014) doi:10.1016/j.cpc.2014.04.012 [arXiv:1310.1921 [hep-ph]].

[60] N. D. Christensen, C. Duhr, B. Fuks, J. Reuter and C. Speckner, Eur. Phys. J. C **72**, 1990 (2012) doi:10.1140/epjc/s10052-012-1990-5 [arXiv:1010.3251 [hep-ph]].

[61] B. Fuks, Int. J. Mod. Phys. A **27**, 1230007 (2012) doi:10.1142/S0217751X12300074 [arXiv:1202.4769 [hep-ph]].

[62] C. Duhr and B. Fuks, Comput. Phys. Commun. **182**, 2404 (2011) doi:10.1016/j.cpc.2011.06.009 [arXiv:1102.4191 [hep-ph]].

[63] N. D. Christensen, P. de Aquino, C. Degrande, C. Duhr, B. Fuks, M. Herquet, F. Maltoni and S. Schumann, Eur. Phys. J. C **71**, 1541 (2011) doi:10.1140/epjc/s10052-011-1541-5 [arXiv:0906.2474 [hep-ph]].

[64] C. Degrande, C. Duhr, B. Fuks, D. Grellscheid, O. Mattelaer and T. Reiter, Comput. Phys. Commun. **183**, 1201 (2012) doi:10.1016/j.cpc.2012.01.022 [arXiv:1108.2040 [hep-ph]].

[65] J. Alwall, M. Herquet, F. Maltoni, O. Mattelaer and T. Stelzer, JHEP **1106**, 128 (2011) doi:10.1007/JHEP06(2011)128 [arXiv:1106.0522 [hep-ph]].

[66] J. Alwall *et al.*, JHEP **1407**, 079 (2014) doi:10.1007/JHEP07(2014)079 [arXiv:1405.0301 [hep-ph]].

[67] P. Skands, S. Carrazza and J. Rojo, Eur. Phys. J. C **74**, no. 8, 3024 (2014) doi:10.1140/epjc/s10052-014-3024-y [arXiv:1404.5630 [hep-ph]].

[68] K. Kong, doi:10.1142/9789814390163-0004 arXiv:1208.0035 [hep-ph].

[69] J. P. Guillaud, CERN-CMS-NOTE-2000-070, CMS-NOTE-2000-070.

[70] T. Sjostrand, S. Mrenna and P. Z. Skands, JHEP **0605**, 026 (2006) doi:10.1088/1126-6708/2006/05/026 [hep-ph/0603175].

[71] M. Cacciari, G. P. Salam and G. Soyez, Eur. Phys. J. C **72**, 1896 (2012) doi:10.1140/epjc/s10052-012-1896-2 [arXiv:1111.6097 [hep-ph]].

[72] M. Cacciari, hep-ph/0607071.

[73] M. Cacciari and G. P. Salam, Phys. Lett. B **641**, 57 (2006) doi:10.1016/j.physletb.2006.08.037 [hep-ph/0512210].

[74] S. Catani, Y. L. Dokshitzer, M. H. Seymour and B. R. Webber, Nucl. Phys. B **406**, 187 (1993). doi:10.1016/0550-3213(93)90166-M

[75] S. D. Ellis and D. E. Soper, Phys. Rev. D **48**, 3160 (1993) doi:10.1103/PhysRevD.48.3160 [hep-ph/9305266].

[76] J. de Favereau *et al.* [DELPHES 3 Collaboration], JHEP **1402**, 057 (2014) doi:10.1007/JHEP02(2014)057 [arXiv:1307.6346 [hep-ex]].

[77] A. Mertens, J. Phys. Conf. Ser. **608**, no. 1, 012045 (2015). doi:10.1088/1742-6596/608/1/012045

[78] H. Baer *et al.*, arXiv:1306.6352 [hep-ph].

[79] H. Baer, M. Berggren, J. List, M. M. Nojiri, M. Perelstein, A. Pierce, W. Porod and T. Tanabe, arXiv:1307.5248 [hep-ph].

[80] G. L. Bayatian *et al.* [CMS Collaboration], J. Phys. G **34**, no. 6, 995 (2007). doi:10.1088/0954-3899/34/6/S01

[81] A. Hocker *et al.*, PoS ACAT , 040 (2007) [physics/0703039 [PHYSICS]].

[82] J. Stelzer, A. Hocker, P. Speckmayer and H. Voss, PoS ACAT **08**, 063 (2008).

[83] J. Therhaag [TMVA Core Developer Team Collaboration], AIP Conf. Proc. **1504**, 1013 (2009). doi:10.1063/1.4771869

[84] P. Speckmayer, A. Hocker, J. Stelzer and H. Voss, J. Phys. Conf. Ser. **219**, 032057 (2010). doi:10.1088/1742-6596/219/3/032057

[85] J. Therhaag, PoS ICHEP **2010**, 510 (2010).

[86] A. L. Read, J. Phys. G **28**, 2693 (2002). doi:10.1088/0954-3899/28/10/313
B. Mistlberger and F. Dulat, arXiv:1204.3851 [hep-ph].

[87] L. Moneta *et al.*, PoS ACAT **2010**, 057 (2010) [arXiv:1009.1003 [physics.data-an]].

[88] S. Khatibi and M. Mohammadi Najafabadi, Phys. Rev. D **89**, no. 5, 054011 (2014) doi:10.1103/PhysRevD.89.054011 [arXiv:1402.3073 [hep-ph]].

[89] FCC-ee (TLEP) Physics Workshop (TLEP9), 3-5 February 2015, PISA, Italy, https://indico.cern.ch/event/357188/.

[90] FCC Week 2015, International Future Circular Collider Conference, March 23-27 2015, Washington DC, USA, http://indico.cern.ch/event/340703/.

[91] FCC-ee (TLEP) Physics meeting, 1 September 2014, CERN, https://indico.cern.ch/event/326783/.

[92] Top Physics Meeting, 12 January 2015, CERN, https://indico.cern.ch/event/358080/.